CHALMERS
UNIVERSITY OF TECHNOLOGY

MODELLING OF THE BATTERY STRESSES IN THE PLUG-IN HYBRID TEST VEHICLE

Master of Science Thesis

Deepika Iyer
Prerna Gupta

The Division of Electric Power Engineering
CHALMERS UNIVERSITY OF TECHNOLOGY
Gothenburg Sweden 2018

Master's thesis June 2018

MODELLING OF THE BATTERY STRESSES IN THE PLUG-IN HYBRID TEST VEHICLE

DEEPIKA IYER
PRERNA GUPTA

CHALMERS
UNIVERSITY OF TECHNOLOGY

Department of Energy and Environment
Division of Electric Power Engineering
Chalmers University of Technology
Gothenburg, Sweden 2018

Modelling of the Battery Stresses in the Plug-in Hybrid Test Vehicle

DEEPIKA IYER
PRERNA GUPTA

Supervisor: Evelina Wikner, Electric Power Department
Supervisor: Johan Scheers, Volvo Cars Corporation
Examiner: Torbjörn Thiringer, Electric Power Department

Master's Thesis June 2018
Department of Energy and Environment
Division of Electric Power Engineering
Chalmers University of Technology
SE-412 96 Gothenburg
Telephone +46 31 772 1000

Printed by Chalmers Bibliotek, Reproservice
Gothenburg, Sweden 2018

Acknowledgements

We would first like to express our sincere gratitude towards our examiner Prof. Torbjörn Thiringer and our supervisor Evelina Wikner at Chalmers University of Technology, for their valuable feedback and suggestions that helped us shape the project. We would also like to thank our supervisor at Volvo Cars Corporation, Johan Scheers for his continuous guidance and support during the project which has been fundamental for completion of the project.

Secondly, we would like to thank our family and friends for their love and support and all other people who have contributed towards the completion of our Thesis work.

Abstract

With the world striving for a clean environment, the use of fossil fuels in vehicles is a rising concern due to its harmful environmental effects. While the possibility of renewable energy is being explored on one side, electrification of vehicles is also becoming increasingly important. Batteries being the chief component, with the increasing demand of electric and hybrid vehicles, understanding of the batteries in terms of ageing and lifetime becomes crucial.

In this thesis, the effect of driving patterns on battery ageing is evaluated and some of the factors contributing to the ageing are identified, so as to be able to prolong the battery life with an economical driving. This evaluation involves building a test vehicle model, developing a battery ageing model, and integrating both of them. The test vehicle under study is a Plug-in hybrid vehicle and its electric mode is built in the Matlab QSS toolbox. Field data from the test vehicle is used to validate the vehicle model i.e. how closely it represents the actual vehicle. A battery ageing model is developed, which is dependant on the Charging rate (C rate) and the State of Charge (SOC) using existing Li-ion cell test data. The vehicle and the ageing model are then integrated and used to study real driving cycles from different customers.

The ageing analysis shows that there is a reduction in the battery capacity as the number of Full cycle equivalent (FCE) increases. The capacity reduction is significant for the higher charging and discharging rates as compared to the lower ones. Moreover, for smaller 10% Depth of Discharge (DOD), the ageing is more prominent at the higher SOC levels than at the lower SOC levels. Different driving patterns affect the battery ageing in different ways. An increase in the average speed by 70% from 47.6 km/hour to 79 km/hour can reduce the battery life-time by nearly 40%. Also, increasing the acceleration limits from $2m/s^2$ to $7m/s^2$ shortens the battery life by 13%. Thus, driving with higher speeds and higher accelerations intensifies the ageing process.

Keywords

Electric Vehicle (EV), Plug-in Hybrid Electric Vehicle (PHEV), Hybrid Electric Vehicle (HEV), Quasistatic Simulation tool box (QSS TB), Full cycle equivalent (FCE), State of Charge (SOC), C rate (Charging rate), DOD (Depth of Discharge).

Contents

Chapter 1

Introduction

1.1 Background

With the rising concern of CO_2 emissions, the world is trying to find more environment friendly solutions. One of the major ways to curb the rising pollution is to use of Hybrid electric vehicles (HEVs) and Electric vehicles (EVs) instead of conventional combustion engine vehicles.

Energy storage systems such as batteries are necessary to power the HEVs and EVs. Battery technology is continuously developing with novel cell chemistries being researched to meet the needs of the automobile industry. The Li-ion battery (LiB) possesses high energy density and requires low maintenance, thus it is dominating the automotive industry. The advancements in the development of the batteries play a key role in increasing the acceptance of the HEVs and EVs. Figure 1.1 shows the electrified vehicles sales in Europe over recent years and the prognosis for the coming years [1]. It shows that the number of hybrid and electric vehicles sold are drastically rising and are estimated to increase further. This justifies the need to study and understand the batteries.

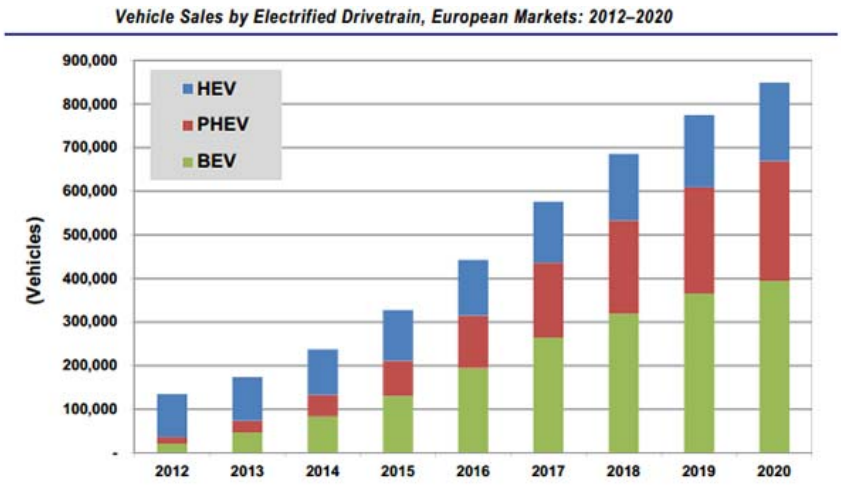

Figure 1.1: Sales of Electrified vehicles in Europe

Understanding the LiBs in terms of ageing and lifetime becomes essential since the battery, based in the high cost, is an irreplaceable part of HEVs and EVs. The purpose of this study is to analyze the battery stresses and various factors which contribute to the battery ageing in order to understand the ways to improve the battery life.

1.2 Purpose of Work

This thesis work is a part of the publicly funded APL project which is a collaboration between Chalmers University of Technology (CTH), Uppsala University (UU), Volvo Car Corporation (VCC) and ABB. The aim of this project is to develop intelligent battery steering based on the knowledge about the battery aging processes to prolong the lifetime of a battery in vehicle application [2].

This thesis is aimed towards the bigger APL goal. The purpose of this work is to study the battery ageing for different driving patterns and identify driving parameters that can accelerate or slow down the ageing. This can help the customers to opt for an economical driving and thus achieve a prolonged battery life.

1.3 Aim

The project aims to develop a Plug-in hybrid test vehicle model in the Quasi Static Simulation Toolbox (QSS TB) along with the battery ageing model in Matlab to study the battery stresses for different drive cycles and thereby identify the factors influencing the life-time of the battery.

1.4 Problem description

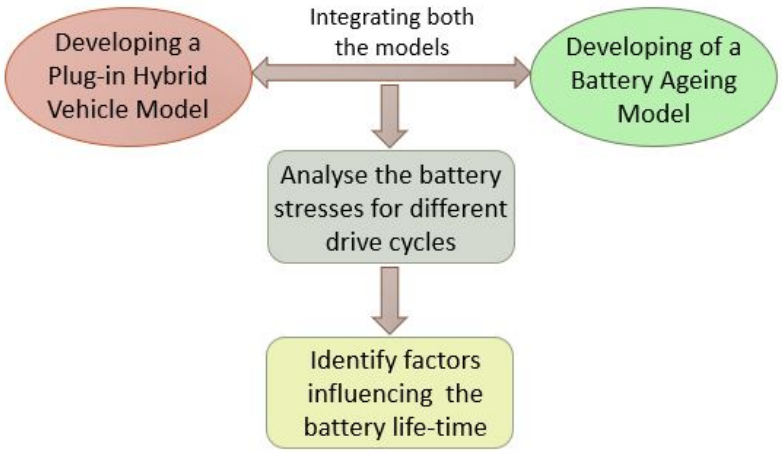

Figure 1.2: Key Steps in the Thesis work

Figure 1.2 shows that the project can be sub-divided into four main problems:

i) Building a complete vehicle model (Electric mode) of the Plug-in hybrid test vehicle
ii) Developing an ageing model of the Li-ion battery
iii) Integrating the vehicle and the battery ageing model
iv) Identifying factors contributing to the battery stresses

An Electric mode of the test vehicle is built using the Matlab QSS toolbox. Field data from the test vehicle and actual driving data from the customers are obtained and compared with the results from the vehicle simulation model, to verify how closely the Simulink model represents the actual vehicle.

The existing Li-ion cell test data are curvefitted and the Capacity degradation over a number of FCEs (Full cycle equivalent) is determined. Thereby, a battery ageing model is built which is dependent on the C rate and SOC. The ageing model is verified using Hyzem driving cycle data.

The vehicle model and the battery ageing models are integrated by discretizing the field driving data to suit the integrated model. The battery parameters and corresponing ageing are studied for various driving patterns.

From the above, the factors contributing to ageing of the batteries are identified, so as to be able to prolong the battery life with economical driving.

1.5 Scope

The project will mainly focus on:

- Modelling the Electric mode of the Plug-in hybrid test vehicle and validate it with respect to the actual test vehicle
- Study and analyze the capacity degradation of a single Li-ion cell from the available test data and thereby develop a battery ageing model
- Verify the battery ageing model using a test cycle
- Integrate the vehicle model and the battery ageing model
- Study and examine the stresses on battery pack during different driving scenarios

Due to time constraint, the project work does not consider the following aspects:

- The study assumes even ageing of all the cells in the battery pack. Thus, it does not cover the impact of uneven cooling and unequal temperature distribution
- The model of the test vehicle does not consider the impact of temperature such as the ambient or the battery temperature
- In a real vehicle, the rolling friction coefficient (C_r) and drag coefficient (C_d) vary as a function of the vehicle speed. However, the test vehicle model uses

an average value of C_r and C_d for the ease of modelling

1.6 Sustainability Aspects

LiB is currently the most promising battery technology used in Electric and Hybrid vehicles. Compared to other battery technologies available in the market, the LiB has many advantages such as high energy density, making it ideal for battery electric vehicles, but there is a sustainability aspect related to the use of these batteries which needs to be addressed by e.g. recycling [3].

The number of electric cars in the world passed the 2 million mark in 2016 and the International Energy Agency estimates there will be 140 million electric cars globally by 2030 if countries are to meet the Paris climate agreement targets. This increase in electric vehicle production could leave 11 million tonnes of spent LiBs that need recycling [3]. Presently, only 5% of the battery waste is recycled. This affects the environment and creates scarcity of precious metals like lithium and cobalt. Thus, efficient and economical recycling must be developed to prevent environmental pollution and to conserve raw material [4].

Due to lack of a specific collection system, there are very few recycling plants in major battery producing countries such as China and Korea. As a consequence, LiBs (after end of life) are treated with a municipal solid waste treatment approach. The overall recycling rate of metals like Fe, Cu, Al, Co, Ni, and Mn are over 50% while the recycling rate of Li is less than 1%. Thus, there is a need to develop a comprehensive and highly efficient process in the near future [4].

Presently, the recycling and recovery of LiBs is very complex, expensive and time consuming. New technologies that reduce the complexity and time for recycling need to be developed for high eco efficiency. Large scale treatment plants need to be established along with efficient collection system from the consumers. It is also essential to create a legislation management system covering the life cycle of LiBs towards a sustainable industry [4].

1.7 Ethics

1. To be honest and realistic in stating claims or estimates based on available data.

The battery ageing model is based on constant current Li-ion data. Thus, there may be a difference in the battery ageing when using a constant current and a dynamic drive cycle. This aspect is highlighted in the report.

2. To improve the understanding of technology; its appropriate application and potential consequences

The ageing model is built taking into account SOC and C rate, ignoring the effect of temperature. It is important to understand that the battery ageing in a real vehicle

may deviate from the thesis results due the effect of temperature.

Chapter 2

Theory

2.1 Different configurations of a Hybrid Electric vehicle

2.1.1 Series Hybrid Drivetrain

In the series hybrid vehicle shown in Figure 2.1, the vehicle is essentially driven by an electric motor. Hence, it needs a high power electric motor to meet the maximum power needs of the vehicle. ICE is provided to enhance the driving range of the vehicle. The ICE and the generator together can either power the motor or charge the battery [5].

Regenerative braking occurs when the motor acts as a generator and provides electrical energy to charge the battery through the inverter. Thus, a series hybrid configuration has the possibility of high regeneration. Since, the ICE does not have to meet the vehicle power requirements, it can always be operated in the region of high efficiency. This in turn curbs the emissions and allows downsizing of the ICE. The major downside of a series configuration is that it requires three machines: an engine, an electric motor and a generator, thereby adding to the overall investment and maintenance cost [5].

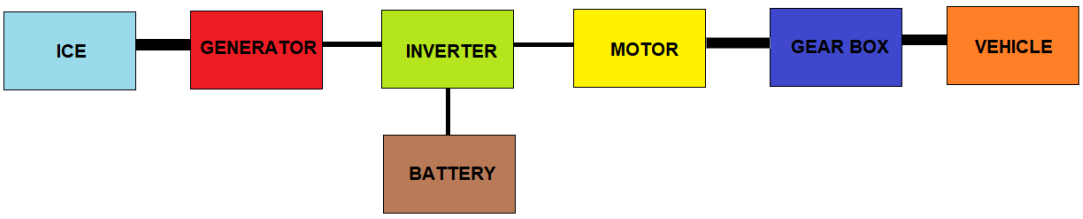

Figure 2.1: Layout of a Series Hybrid Vehicle

2.1.2 Parallel Hybrid Drivetrain

In the parallel hybrid vehicle shown in Figure 2.2, the ICE and the electric motor can drive the vehicle independently or together. Thus, the ratings of the ICE and the electric motor are chosen such that they meet the vehicle power needs together, which results in smaller machines. Parallel hybrid is essentially ICE propelled, where the electric motor acts as a power assist. During the regenerative braking, the electric motor runs as a generator to provide charge to the battery [5].

A parallel hybrid configuration allows the ICE to be turned off at idle. Also, it helps to avoid the ICE operation in low efficiency regions, thus helping to save fuel and reduce emissions. Compared to a series hybrid, the parallel hybrid requires one machine lesser. However, it requires a complex controller design, adding to the overall cost and complexity of the system [5].

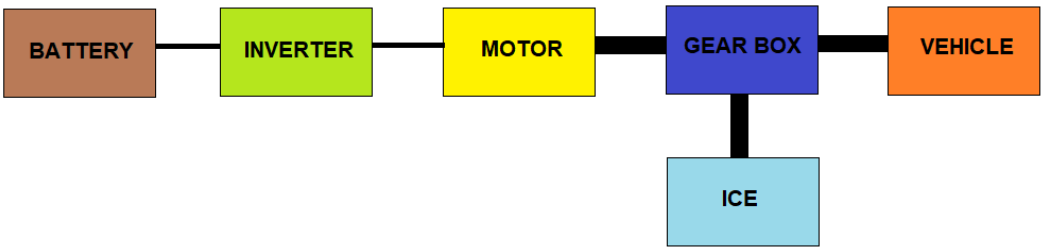

Figure 2.2: Layout of a Parallel Hybrid Vehicle

2.1.3 Series-Parallel or Combined Hybrid Drivetrain

The Combined hybrid power train shown in Figure 2.3 is an transitional configuration between the series and the parallel hybrids. It is primarily a parallel hybrid with some extra properties of a series hybrid. By combining them, the ICE can propel the vehicle directly like in a parallel configuration. At the same time, the ICE can also be disengaged as in a series configuration [5].

Thus the Combined hybrid offers the merits and demerits of both the series and parallel configurations. It is dearer than a parallel hybrid, since it requires an extra generator and a more intricate control system, but it can give a superior performance and higher efficiency than a series or a parallel alone [5].

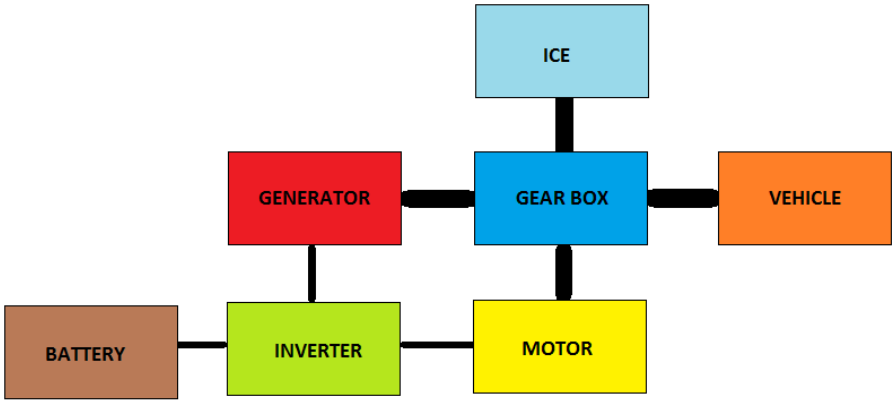

Figure 2.3: Layout of a Series-Parallel Hybrid Vehicle

2.2 Series-parallel Hybrid Test Vehicle

Figure 2.4 shows the component layout of the Series-Parallel PHEV test vehicle under study. As can be observed, the ICE and the electric generator (EG) are mounted on the front axle and drive the front wheels of the vehicle. While the electric motor (EM) drives the rear wheels of the vehicle. The battery can either power the electric motor or can be recharged from the ICE and the EG, depending on its SOC limits. The inverter converts the power from dc to ac or vice versa.

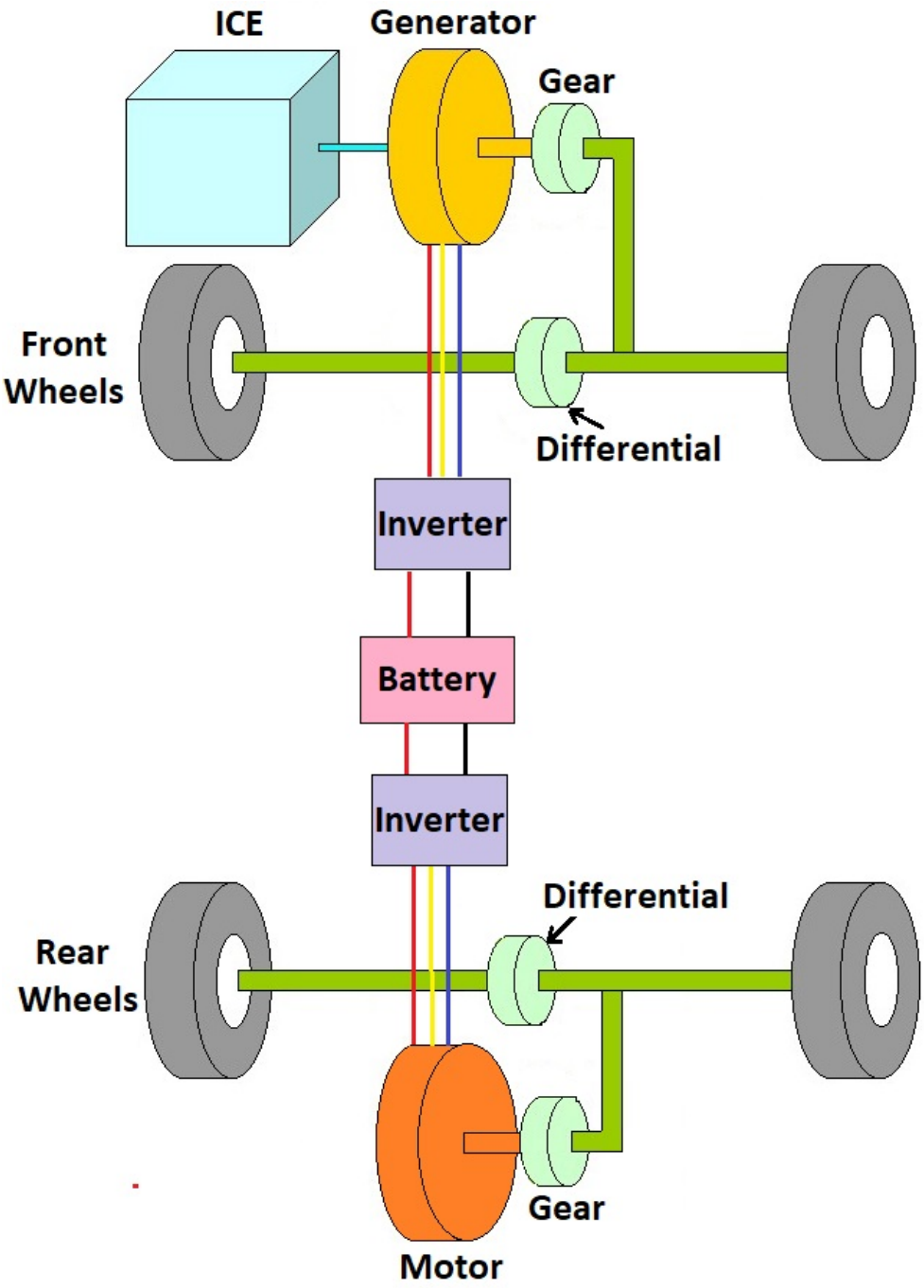

Figure 2.4: Component layout of Series-Parallel Test Vehicle

2.3 Different modes of a Series-parallel Hybrid vehicle

A Series-Parallel hybrid vehicle can function in any of the following modes:

2.3.1 Pure Electric Mode

In the pure electric mode shown in Figure 2.5, the battery powers the electric motor through the inverter and the motor in turn propels the vehicle [5]. This is the cleanest and most efficient operation mode requiring no fuel.

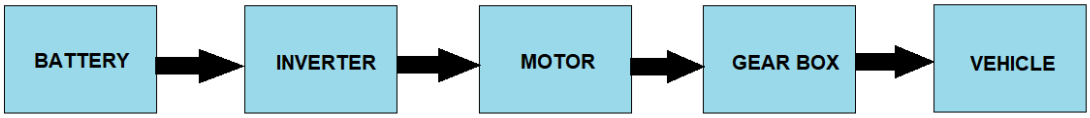

Figure 2.5: Pure Electric mode

2.3.2 Internal Combustion Engine (ICE) Mode

In the ICE mode shown in Figure 2.6, the ICE powers the vehicle through the transmission [5]. This is the conventional mode producing high emissions.

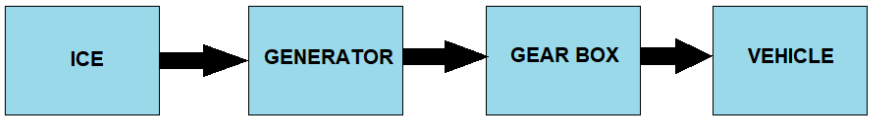

Figure 2.6: ICE mode

2.3.3 ICE Recharging Mode

In this mode, the ICE drives the vehicle as well as charges the battery through the electric generator and the inverter as shown in Figure 2.7 [5]. The vehicle operates in this mode when the battery SOC is low and needs to be recharged. This mode calls for highest fuel consumption.

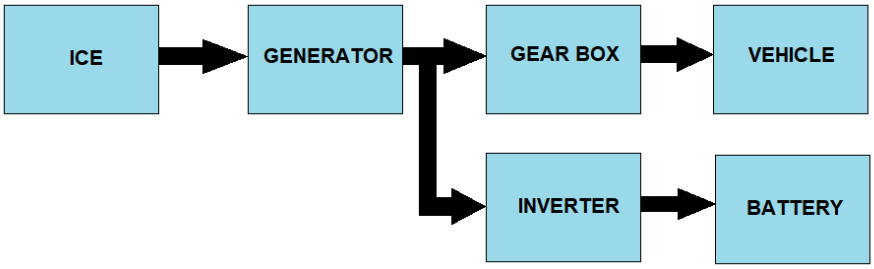

Figure 2.7: ICE Recharging mode

2.3.4 Power Assist Mode

The Power assist mode occurs during high power requirements such as uphill driving or acceleration. During this, both the electric motor and the ICE together propel the vehicle as shown in Figure 2.8 [5].

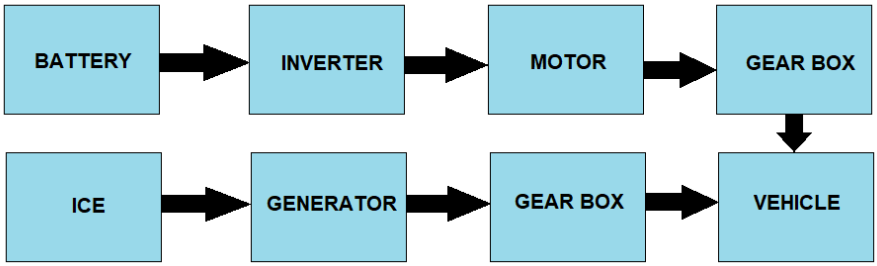

Figure 2.8: Power Assist mode

2.3.5 Regeneration Mode

In this mode, the energy during braking is captured and the generator recharges the battery as shown in Figure 2.9 [5]. This mode helps to capture the braking energy which otherwise gets wasted in the conventional vehicle.

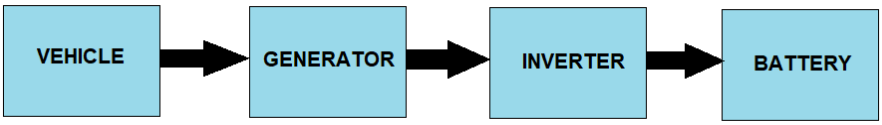

Figure 2.9: Regeneration mode

Chapter 3

Modelling of the Test Vehicle and the Battery Ageing

3.1 Modelling of the Series-Parallel Plug-in Hybrid Test vehicle: Electric Mode

A model of the test vehicle is built in the Matlab QSS TB using the quasi static approach or backward modelling. In this approach, it is assumed that the speed and the acceleration required by the vehicle are already known and based on these the operating conditions of various components like the electric motor and the gear box are calculated. At the end of the simulation, the change in the battery state of charge (SOC) is calculated for the driving cycle.

The Series-Parallel Plug-in hybrid test vehicle operating in the Electric mode is built in the Matlab QSS TB as shown in Figure 3.1. The key components of the system are the vehicle, the transmission, the electric motor and the battery. For a particular driving pattern, the test vehicle having certain properties demands a power which is supplied by the battery. The individual components of the vehicle are governed by some equations which are explained in Section 3.1.1 below.

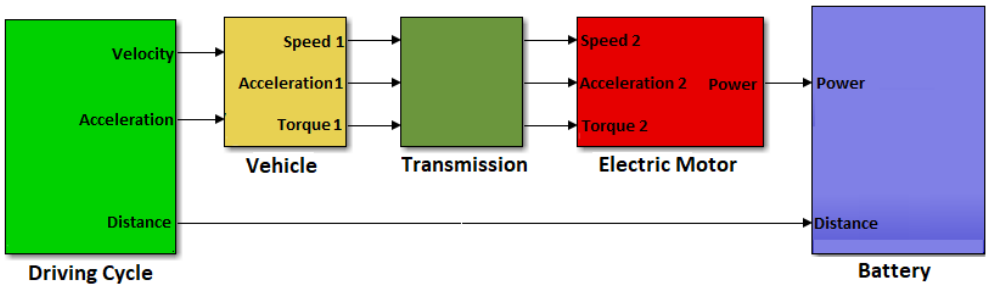

Figure 3.1: Vehicle Model (Electric Mode) in Matlab QSS TB

3.1.1 Key components in the Electric Vehicle Model

3.1.1.1 Vehicle model

There are various types of forces acting on a moving vehicle. Figure 3.2 illustrates the external forces acting on a vehicle to oppose the direction of motion. These are:

a) The aerodynamic force F_a
b) The rolling resistance force F_r
c) The gradient force F_g

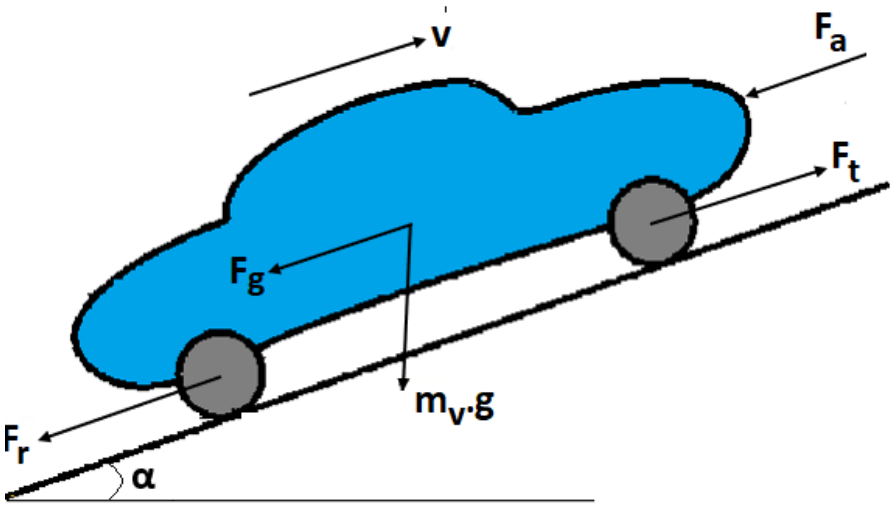

Figure 3.2: Forces acting on a vehicle in motion

a) **Aerodynamic force**

The aerodynamic force acting on a moving vehicle is given by

$$F_a = \frac{1}{2}\rho_a A C_d v^2 \tag{3.1}$$

where ρ_a is the air density, A is the vehicle frontal area, v is the vehicle velocity and C_d is the aerodynamic drag coefficient [5]. Thus, the aerodynamic force increases with the velocity and frontal area. In reality, C_d is a function of velocity but for ease it is assumed to be a constant in this model.

b) **Rolling resistance force**

The rolling resistance force acting on a vehicle is given by

$$F_r = C_r mg \cos\alpha \tag{3.2}$$

where C_r is the rolling friction coefficient, g is the gravitational acceleration, m is the mass of the vehicle and α is the road inclination angle [5]. The rolling friction C_r is a function of velocity, tyre pressure, tyre material and road surface, but in this model it is assumed to be a constant.

c) **Gradient force**

The gradient force acting on a vehicle moving on an inclined surface is given by

$$F_g(\alpha) = mg \sin\alpha \tag{3.3}$$

The gradient force is directly proportional to the mass and sine of road angle [5]. For small road angles, this force does not contribute significantly.

Acceleration force

It is the force required to accelerate the vehicle and is given by

$$F_{acc} = m\frac{dv}{dt} \tag{3.4}$$

The acceleration force is directly proportional of the mass of the vehicle and the derivative of velocty with respect to time i.e. the acceleration required [5].

Traction force

The traction force is the net force which needs to be produced in order to move the vehicle forward. It is a combination of all the opposing forces and the acceleration force [5].

$$F_t = F_{acc} + (F_a + F_r + F_g) \tag{3.5}$$

Higher the opposing forces, greater is the traction force required to propel the vehicle.

3.1.1.2 Transmission model

The transmission or gear box is used to convert the electric motor power at a speed w_m and torque T_m to the vehicle speed w_v and torque T_v such that

$$w_m = w_v n \tag{3.6}$$

$$T_v = T_m n \tag{3.7}$$

where n is the gear or the transmission ratio [5].

3.1.1.3 Electric Machine model

In the quasi static model of the electric machine, the input to the electric machine block are the angular wheel speed w_v, the angular acceleration dw_v and the wheel torque T_v. Based on the machine efficiency map, the required machine power P_m is calculated as the output of this block. Positive power indicates that the machine works as an electric motor and negative power means that it works as an electric generator. The electric motor output power is thus given by

$$P_m = \frac{T_m w_m}{\eta_m} \tag{3.8}$$

where P_m is the electrical motor power, T_m is the motor torque, w_m is the motor speed, the product of $T_m w_m$ is the mechanical power and η_m is the efficiency of the machine at a point of operation [5].

3.1.1.4 Battery model

The data from the actual test of a Li-ion cell is used to develop the battery model from the Open Circuit Voltage (OCV) curve as shown in Figure 3.3. The OCV is defined as the state where no net current flows through the battery as the two terminals are not connected.

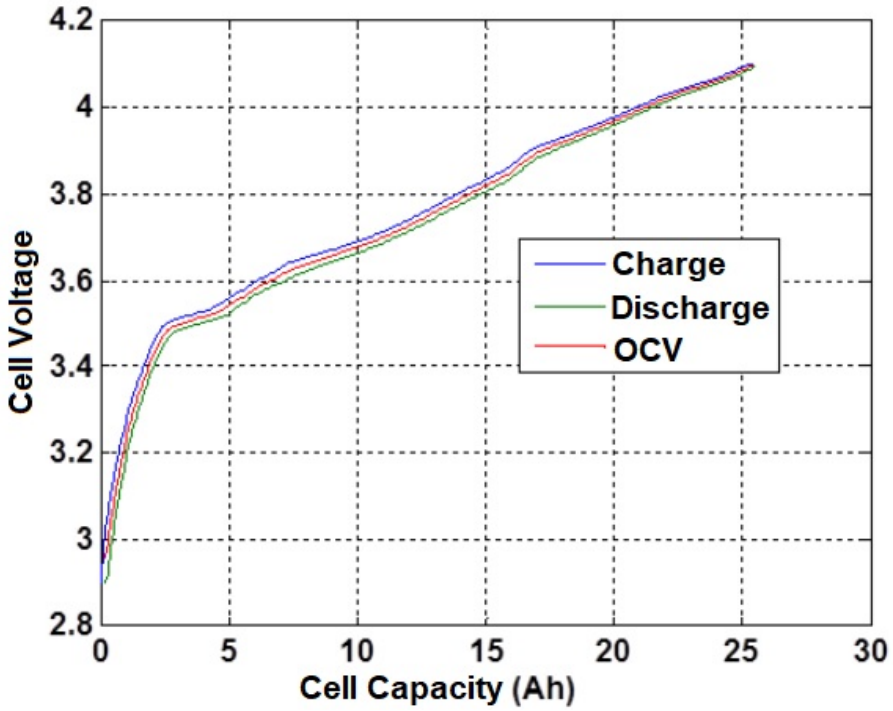

Figure 3.3: Open Circuit Voltage (OCV) curve of a Li-ion cell

Using the curve fit function in Matlab, the open circuit voltage is calculated as

$$V_{ocv} = a * e^{(-b \int i.dt)} + c + (d \int idt) \tag{3.9}$$

where V_{ocv} is the open circuit voltage of a single cell (V), $\int idt$ is the actual cell charge (Ah), and a, b, c and d are constants whose values depend on a particular cell type [6].

For this particular Li-ion cell, the value of these constants are a= -0.6012, b= 0.00032, c= 3.408 and d= 7.64e^{-6}.

The terminal voltage of a single cell can be calculated as

$$V_T = V_{ocv} - iR_{Batt} \tag{3.10}$$

where R_{Batt} is the internal resistance and i is the current flowing through the cell.

The terminal voltage of the battery changes according to the number of cells connected in series or parallel.

3.1.2 Model specifications

The parameters of the different components used in the modeling of the Electric test vehicle such as the Vehicle, Transmission, Motor and Battery are specified in this section.

3.1.2.1 Vehicle parameters

The specifications of the test vehicle being studied are summarized below in Table 3.1.

Table 3.1: Vehicle Specifications

Parameters	Value
Total Mass	2300 kg
Rotating Mass	5 percent
Cross Section	2 m^2
Wheel Diameter	0.724 m
Drag Coefficient	0.3
Rolling Friction Coefficient	0.015

The efficiency of transmission in the test vehicle is assumed to be 98 percent. Hence, the value of drag and rolling friction coefficients C_d and C_r respectively, specified in the Table 3.1 are chosen corresponding to 98 percent efficiency, as depicted in the Figure 3.4 below.

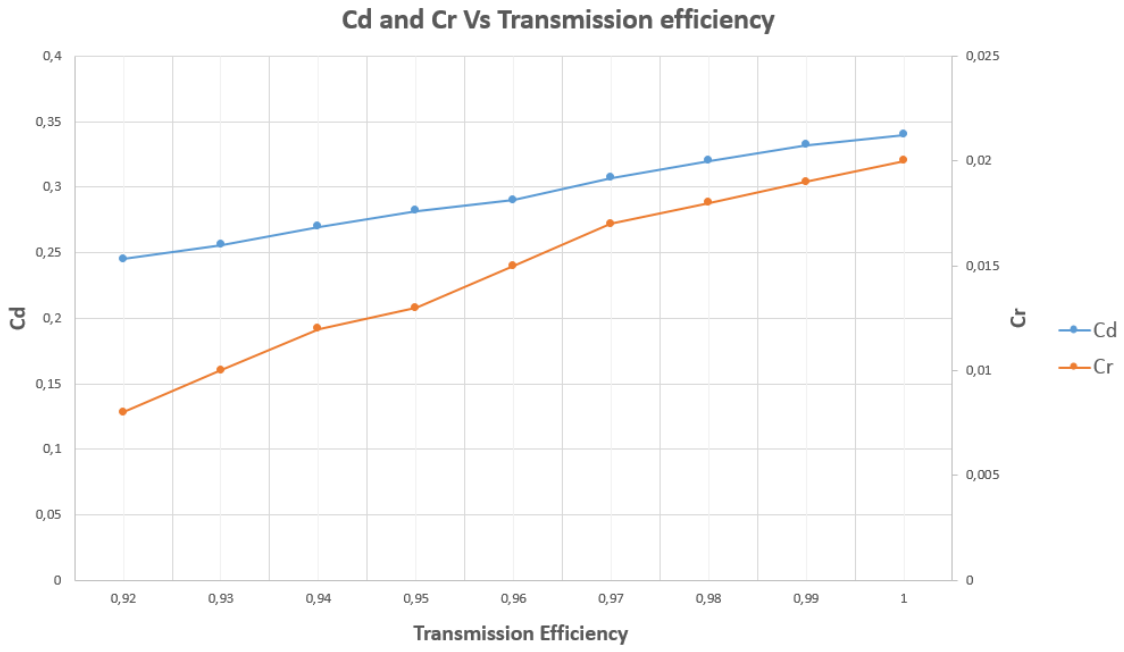

Figure 3.4: Drag Coefficient and Rolling Resistance Vs Efficiency

The variation of Drag coefficient(C_d) and Rolling resistance Coefficient(C_r) with the Vehicle transmission efficiency (η) can be seen from the Figure 3.4. As the transmission efficiency (η) is reduced from 100 to 92 percent, the output or the

propulsion power from the Electric machine drops. In turn, the traction force F_t reduces. To maintain the required acceleration force F_a, the opposing forces F_r and F_a reduces i.e. lower C_r and C_d values as can be observed in the Figure 3.4 above.

3.1.2.2 Gear parameters

The specifications of the transmission system used for the electric motor are summarized below in Table 3.2

Table 3.2: Transmission Specifications

Parameters	Value
Type	Fixed Gear
Gear Ratio	10
Efficiency	0.98
Idling losses	0 W

3.1.2.3 Motor parameters

The specifications of the Electric motor are summarized below in Table 3.3

Table 3.3: Electric Motor Specifications

Parameters	Value
Maximum Power	60 kW
Maximum Torque	250 Nm
Maximum Speed	14000 rpm
Nominal Speed	3200 rpm

The efficiency map of the electric motor used in the actual test vehicle is as shown in Figure 3.5. This map is derived from the actual vehicle testing data and is fed into the QSS vehicle model.

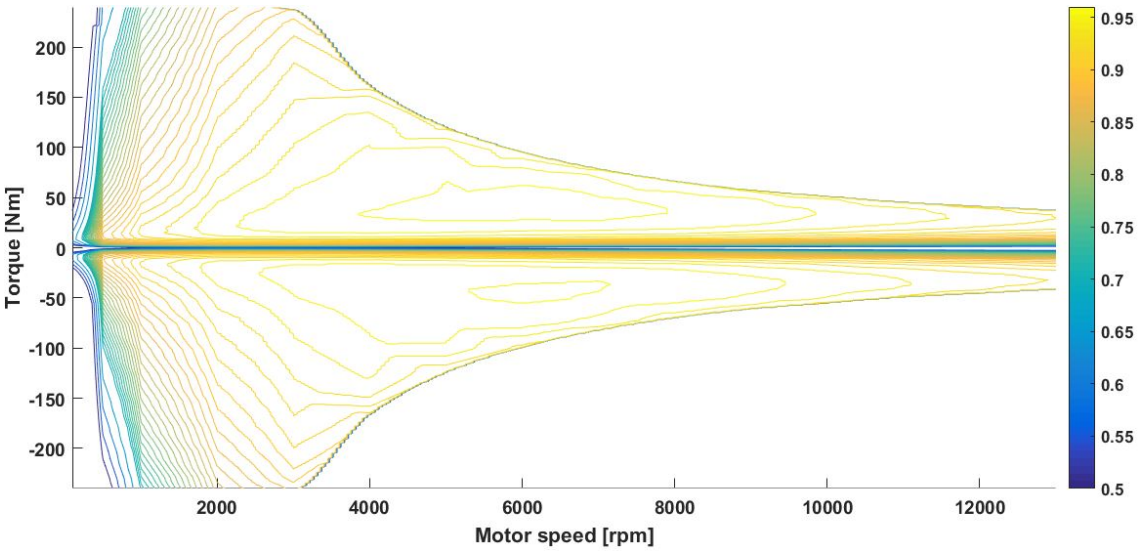

Figure 3.5: Efficiency map of the electric motor in test vehicle

3.1.2.4 Battery parameters

The specifications of the Battery used in the test vehicle are summarized below in Table 3.4

Table 3.4: Battery Specifications

Parameters	Value
Type	Lithium-Ion
Cell Voltage	3.65 V
Internal resistance	0.002 Ω
Cell capacity	26 Ah
Number of series connected cells	96
Number of parallel connected cells	1
Total number of cells	96
Battery total capacity	2.5 kAh

3.2 Modelling and Analysis of the Battery Ageing

The Battery is the most critical component in an electric and hybrid car, which is why the battery ageing and life time analysis is of great importance. The ageing of a battery is a very complex issue since even a small change in the operating parameters can affect the battery's lifetime and therefore influence its cost.

3.2.1 Empirical Battery Ageing Model

An empirical model for the Li-ion battery has been developed based on the existing Li-ion cell testing data [6]. This ageing model is mainly dependent on two battery parameters- SOC and C-rate.

The battery ageing model must be able to predict the capacity degradation with the increase in the number of Full cycle equivalent (FCEs). Three models have been developed to determine the battery capacity reduction with respect to FCE based on SOC and C-rate as follows:

1) Capacity degradation dependent on SOC
2) Capacity degradation dependent on C-rate
3) Capacity degradation dependent on SOC and C-rate combined

3.2.1.1 Capacity degradation dependence on SOC

The cell capacity does not remain the same with the increase in the number of charge and discharge cycles (FCEs) and this behaviour is affected by the battery SOC level. To analyze this, the entire SOC window of 0-90% is divided into intervals of 10% DODs and capacity degradation cycling in each interval is observed.

By curve-fitting the cell testing data, the cell capacity (Cap) can be expressed in terms of FCE by an exponential expression,

$$Cap = a_1 e^{b_1 FCE} + c_1 \tag{3.11}$$

where a_1, b_1 and c_1 are the ageing functions.

Using curve fitting, the ageing functions can be expressed with respect to SOC by the following single order polynomial expressions,

$$a_1 = a_{11} SOC + a_2 \tag{3.12}$$

$$b_1 = constant = -0.00067 \tag{3.13}$$

$$c_1 = c_{11} SOC + c_{12} \tag{3.14}$$

where $a_{11} = 2.725, a_{12} = 2.25$,$c_{11} = -2.756$ and $c_{12} = 98.56$.

Thus, using the above relations, the Capacity can be calculated for different SOC levels from (3.11). This calculated capacity can be plotted with the measured capacity for different SOC windows for 2C rate as shown in Figure 3.6.

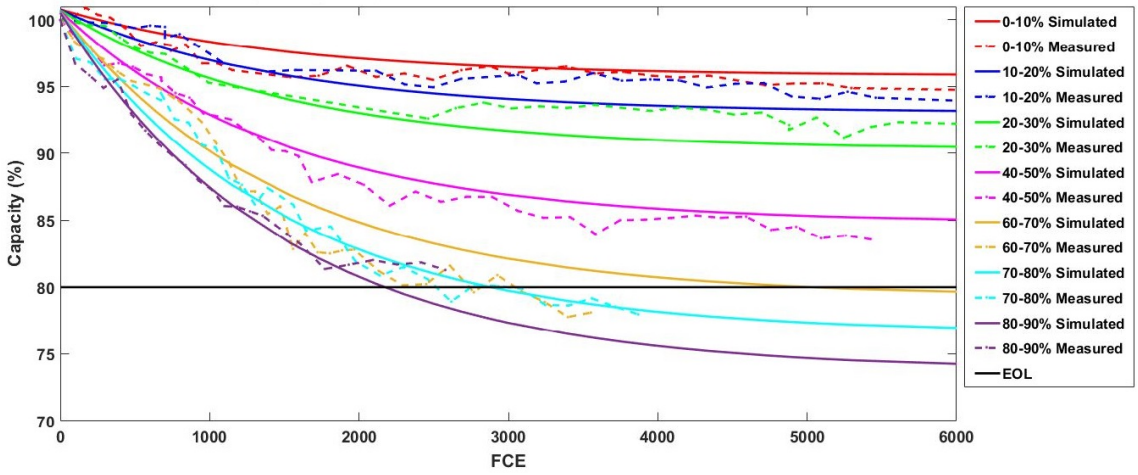

Figure 3.6: Capacity degradation for different SOC levels for 2C

From Figure 3.6, it can be observed that the calculated capacity for different SOC levels are in line with the measured capacity. It can also be noted that the capacity is reduced as the number of FCE increases. Also, this capacity drop is more significant for higher SOC windows as compared to the lower ones. Considering an end of the battery life at 80% capacity, it can be observed that for higher SOC ranges (beyond 60%), the end of life (EOL) is reached much earlier than at lower SOC levels.

3.2.1.2 Capacity degradation dependence on C-rate

The cell ageing is dependent on the charge and the discharge rates of the battery. The capacity degradation model is developed for four different charging rates- 1C, 2C, 3C and 4C by curve fitting the cell testing data for 20-80% SOC window at different C-rates. The cell capacity (Cap) can thus be expressed as

$$Cap = a_2 e^{b_2 FCE} + c_2 \tag{3.15}$$

where a_2, b_2 and c_2 are the ageing functions.

The ageing functions are dependent on the C-rate and can be expressed as

$$a_2 = a_{21} Crate + a_{22} \tag{3.16}$$

$$b_2 = constants \tag{3.17}$$

$$c_2 = c_{21} Crate + c_{22} \tag{3.18}$$

where the values of the constants are: $a_{21} = 23.78, a_{22} = -12.74, c_{21} = -24.39, c_{22} = 39.4$.

Using the above relations, the capacity can be calculated for different C-rates and a fixed SOC window from (3.15). The calculated capacity can be plotted with the measured capacity for different C-rates and 20-80% SOC window as shown in Figure 3.7.

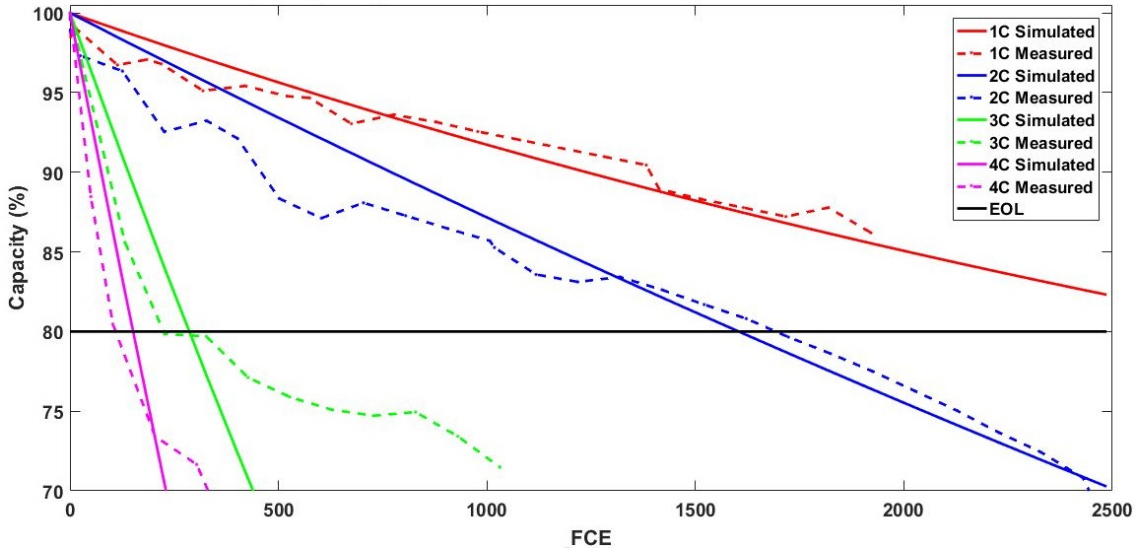

Figure 3.7: Capacity degradation for different C-rates for 20-80% SOC

Figure 3.7 shows that the simulation results almost follow the measured test data. The reduction in the cell capacity is more significant at higher C-rates as compared to the lower ones.

3.2.1.3 Capacity degradation dependence on C-rate and SOC

In the real world, both SOC and C-rate can affect the battery simultaneously. Thus, an ageing model is developed for different charging rates as well as SOC windows.

By curve fitting the cell test data, the cell capacity (Cap) as function of SOC and C-rate can be expressed as

$$Cap = a_3 e^{(b_3 FCE)} + c_3 \tag{3.19}$$

where a_3, b_3 and c_3 are the ageing functions.

The ageing functions are dependent on C-rate and SOC and can be expressed as

$$a_3 = a_{31} + a_{32}SOC + a_{33}Crate + a_{34}SOCCrate + a_{35}Crate^2 + a_{36}SOCCrate^2 \tag{3.20}$$

$$b_3 = b_{31} + b_{32}Crate + b_{33}Crate^2 \tag{3.21}$$

$$c_3 = c_{31} + c_{32}SOC + c_{33}Crate + c_{34}SOCCrate + c_{35}Crate^2 + c_{36}SOCCrate^2 \tag{3.22}$$

where $a_{31}, a_{32}, a_{33}, a_{34}, a_{35}, a_{36}, b_{31}, b_{32}, b_{33}, c_{31}, c_{32}, c_{33}, c_{34}, c_{35}$ and c_{36} are constants shown in Table 3.5.

Table 3.5: Values of constants for ageing model dependant on SOC and C-rate

Constants	Value
a_{31}	-24.26
a_{32}	16.38
a_{33}	19.27
a_{34}	-10.1
a_{35}	-3.006
a_{36}	1.638
b_{31}	0.0007333
b_{32}	-0.000945
b_{33}	0.0001217
c_{31}	122.9
c_{32}	-16.38
c_{33}	-17.26
c_{34}	10.05
c_{35}	2.538
c_{36}	-1.622

Using the above relations, the capacity can be calculated for different C-rates and SOC windows from (3.19).

There are two scenarios of different DODs considered in this case:

i) Capacity degradation for different C-rates at 10% DODs

ii) Capacity degradation for different C-rates at 60% DOD

i) **Capacity degradation for different C-rates at 10% DODs**

Figure 3.9 shows the simulated and measured capacity for different C-rates for two different 10% DODs, i.e. 10-20% SOC and 60-70% SOC. From Figure 3.9, it can be seen that the calculated capacity for different C-rates and SOC are in line with the measured capacities. It can also be noted that the capacity reduction is drastic for higher SOC windows and higher charging rates.

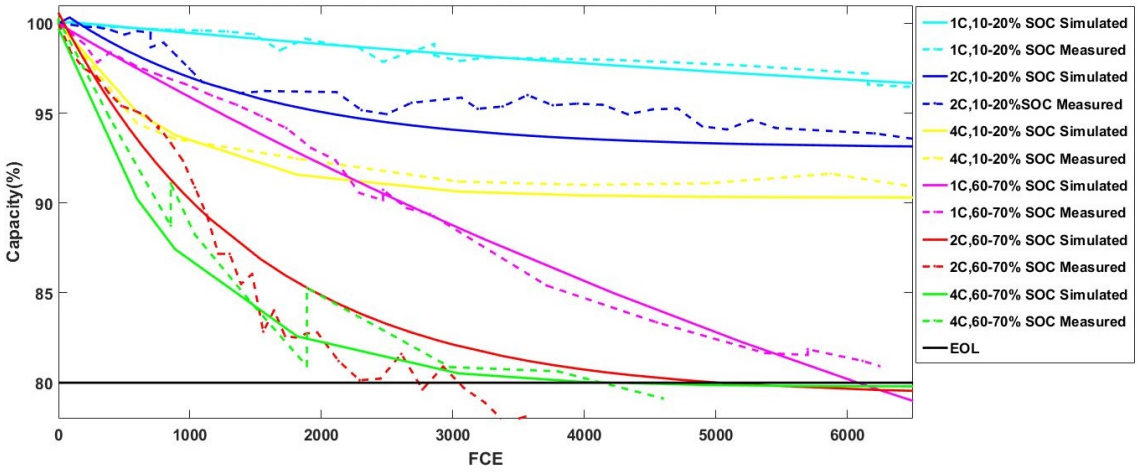

Figure 3.8: Capacity degradation for different C-rates at 10% DODs

ii) **Capacity degradation for different C-rates at 60% DOD**

Figure 3.9 shows the simulated and measured capacity for different charging rates and 60% DOD i.e. 20-80% SOC window. From Figure 3.9, it can be observed that the calculated capacity for 1C and 2C are in line with the measured capacity. However, this model is not valid for higher C-rates (above 2C). This is because in case of 10% DOD, high C-rates appear as current pulses of short duration. However, in case of 60% DOD, high C-rates are currents of longer duration. Since the ageing model is designed for short high current pulses and not long duration high currents, the model cannot accurately predict the capacity degradation for higher C-rates at larger DODs.

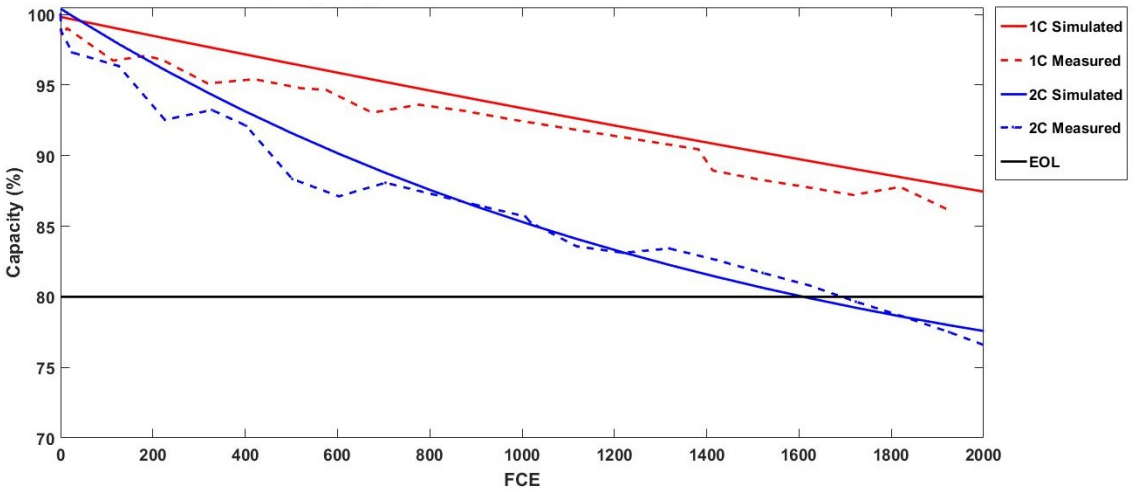

Figure 3.9: Capacity degradation for different C-rates at 60% DOD

Chapter 4

Results and Discussions

4.1 Verification of the Battery Ageing Model and Vehicle Model

4.1.1 Verification of the Battery Ageing Model

The Hyzem drive cycle with 2C RMS discharge and 1C charge current is used to validate the battery ageing model. Figure 4.1 shows the battery current and speed profiles of the Hyzem drive cycle.

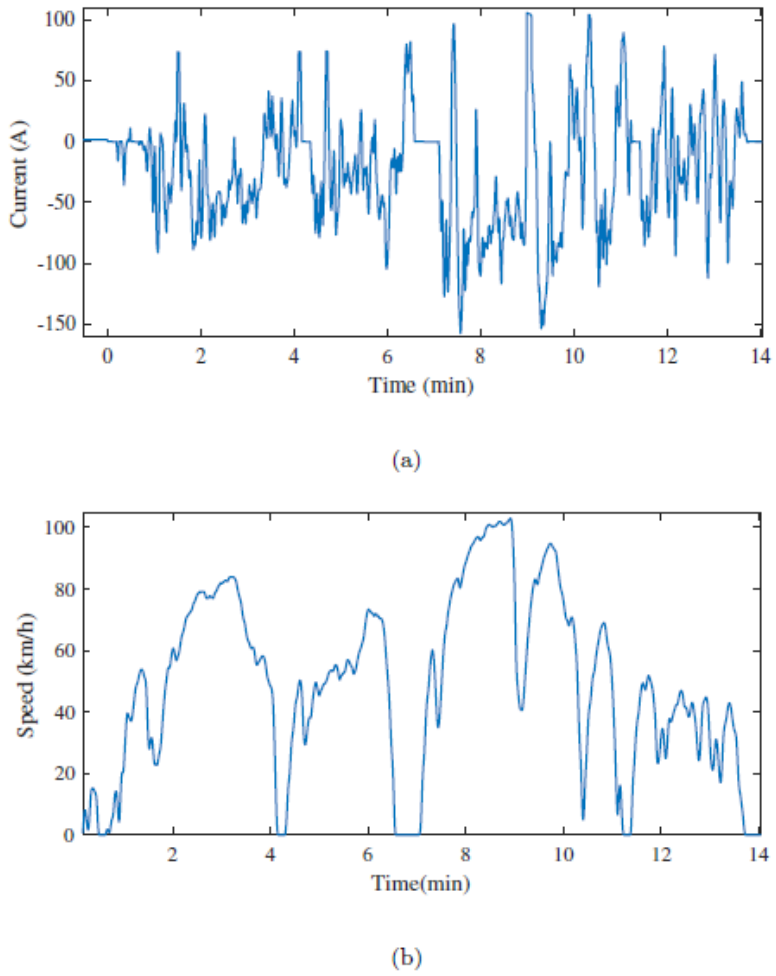

Figure 4.1: Hyzem drive cycle: (a) Battery Current Profile (b) Speed profile

A RMS (Root Mean Square) current method is used for this purpose. The Hyzem drive cycle with a speed varying at each instant fed into the vehicle model results in a varying battery current to be drawn. Thus, at each instant of speed variation,

the battery is being discharged at different rates. To predict the battery capacity degradation due to this drive cycle, the battery current needs to be processed and fed into the ageing model. There are three ways of processing the battery current.

1) **Complete RMS i.e. RMS of the entire current duration**:
In this process, a large number of discharge current values are converted into one RMS value to be fed into the ageing model. This is similar to a constant current being fed into the model. This is the simplest and the easiest process and is quite accurate for nearly constant speed drive cycles. However, for a variable speed driving, this method could underestimate the ageing, since the high C-rates occurring at various instances might be neglected. Thus, in such cases it is important to consider the effect of instantaneous discharging rates.

2) **Discharge current at each instant**:
The ageing model could be made accurate by feeding the instantaneous discharge current. However, these will be very short pulses which may cause the ageing model to behave inaccurately (since the ageing model has been developed for short currents durations corresponding to 10% DODs and not instantaneous pulses). Also, the longer the drive cycle, the more the data points, making the process cumbersome. Hence, this method is not recommended.

3) **Discretized RMS**:
This method is a trade off between the two methods above. In this process, the drive cycle is split into a number of intervals and RMS current values are obtained for each of these intervals. The interval length should be optimized to have an accurate functioning of the ageing model. This method is highly recommended for long variable speed drive cycles since it overcomes the limitations of the above methods.

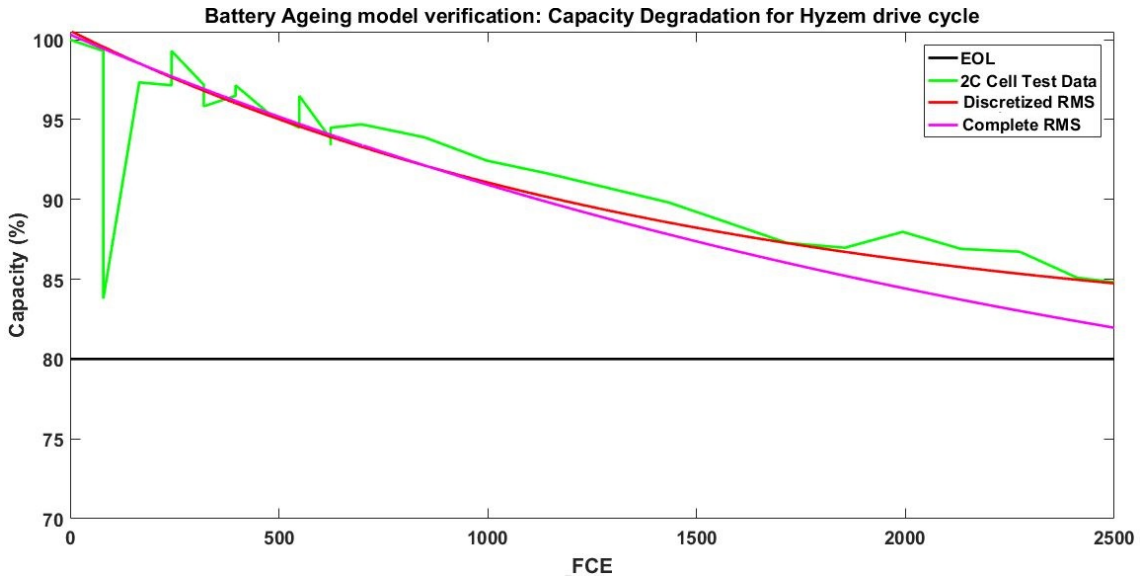

Figure 4.2: Battery Ageing Model verification for Hyzem drive cycle

The capacity degradation from the ageing model is calculated for both Complete

and Discretized RMS currents and is compared with the 2C cell testing data as shown in Figure 4.2. As observed in Figure 4.2, there is a small deviation between the Complete and Discretized RMS and that the Discretized RMS is less aggressive than the Complete RMS. This is beacause it divides the cycle into various intervals whose RMS current value can be higher or lower than constant 2C current.

It is also important to understand that the capacity degradation in the Discretized RMS method is highly dependant on the discretization interval. The more optimum the interval is, the more accurate the ageing model prediction will be.

4.1.2 Verification of the Vehicle Model

The field data is used to check and validate the vehicle simulation model. The field driving cycles comprise of driving at constant speeds with intermediate accelerations or decelerations. For these driving patterns, the battery data of interest, such as the battery current and the battery power, are extracted from the Simulink model and compared with the actual results. Before the field test, it is ensured that the pressure of all the tyres are kept the same (so as to minimize the variations in C_r).

Following are the results of the two field driving data events.

a) Field driving cycle 'A'

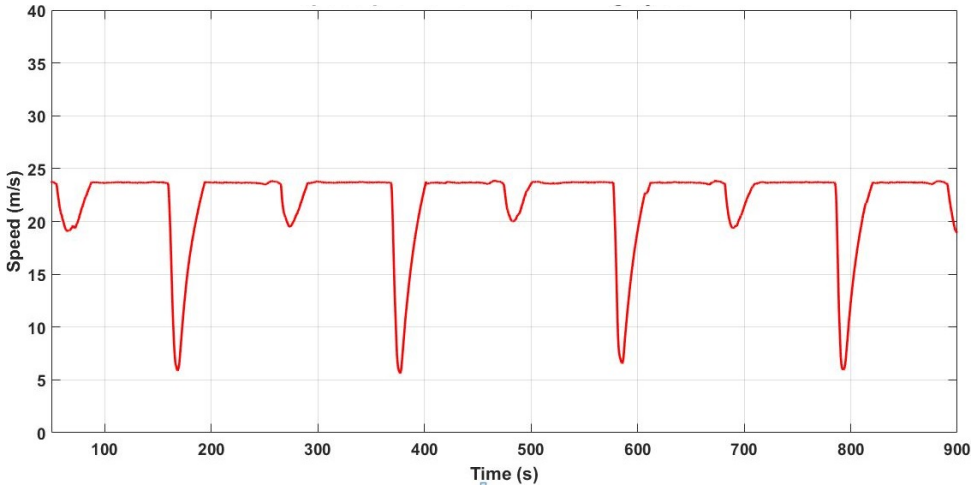

Figure 4.3: Speed profile of the field driving cycle 'A'

Figure 4.3 shows the speed profile of the field driving cycle 'A'. For a major duration, the speed remains constant at around 24 m/s(87km/h) with intermediate decelerations. For the field driving cycle 'A', the battery current and power from the simulink model are compared with the current and power from the actual test vehicle as shown in Figure 4.4 and Figure 4.5.

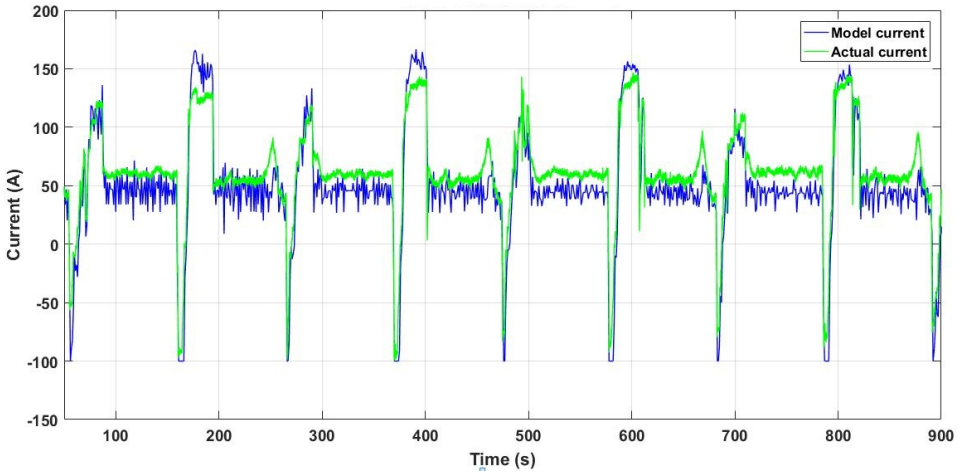

Figure 4.4: Battery current comparison for the field driving cycle 'A'

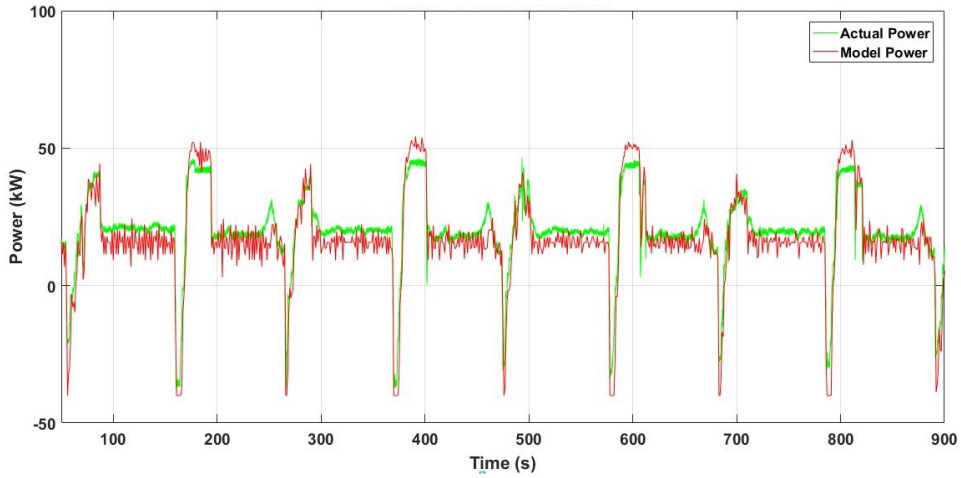

Figure 4.5: Battery power comparison for the field driving cycle 'A'

b) Field Driving cycle 'B'

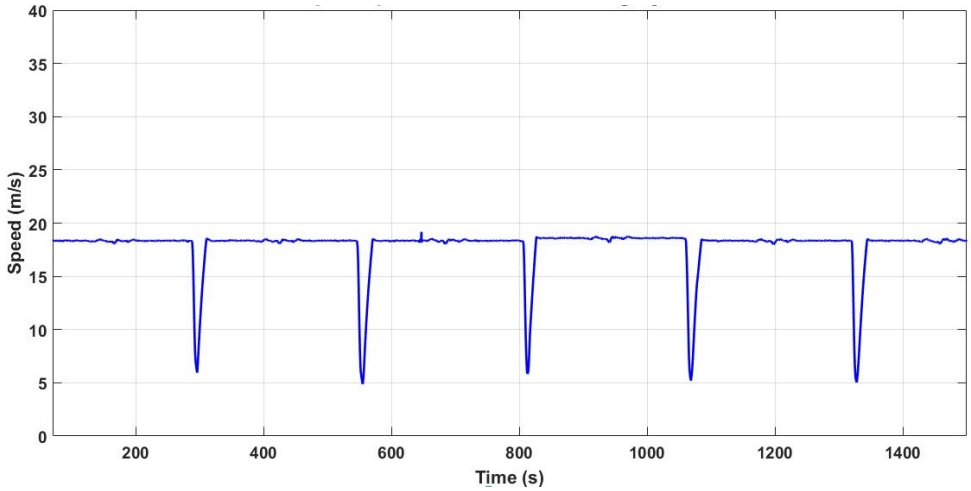

Figure 4.6: Speed profile of the field driving cycle 'B'

Figure 4.6 shows the speed profile of the field driving cycle 'B'. The speed profile

shows that the speed remains constant at around 18.5 m/s(67km/h) for majority period with some intermediate decelerations.

For the field driving cycle 'B', the battery current and power from the simulink model are compared with the current and power from the real vehicle as shown in the following Figure 4.7 and Figure 4.8.

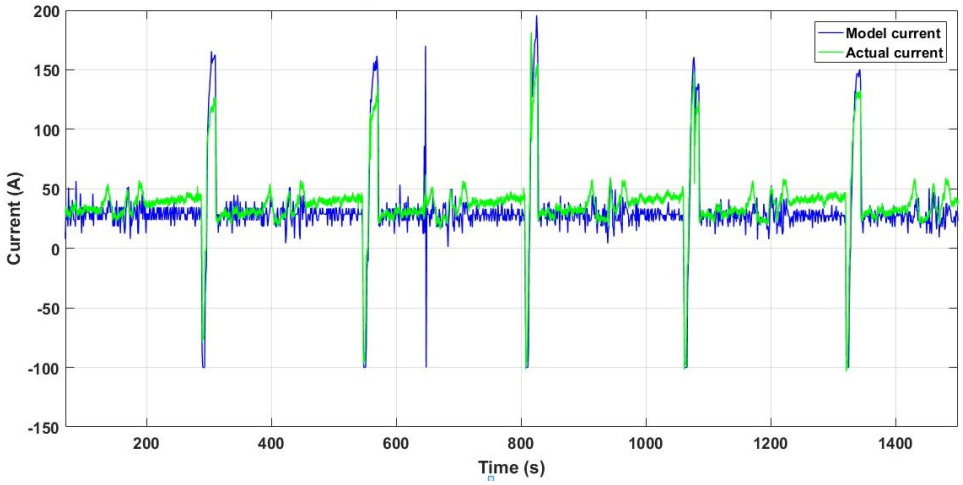

Figure 4.7: Battery current comparison for the field driving cycle 'B'

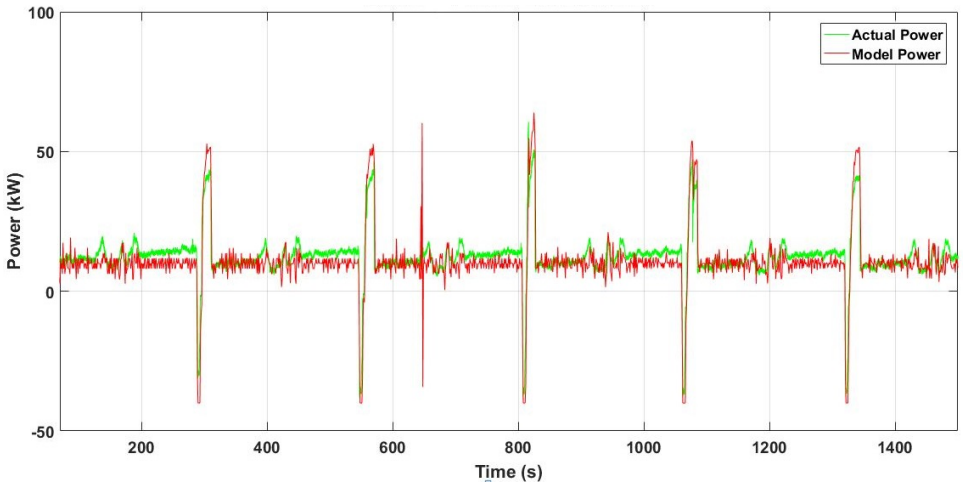

Figure 4.8: Battery power comparison for the field driving cycle 'B'

As can be observed from the Figures above, the battery current and the battery power from the simulink model closely match the actual vehicle current and power for both the drive cycles. The deviations could further be minimized by considering the variation of C_r and C_d with respect to speed. Thus, the above results validate the simulink model to closely represent the actual test vehicle.

4.2 Integration of the Vehicle Model and the Battery Ageing Model

The vehicle model and battery ageing model are integrated and the battery ageing is analysed for field driving cycle 'A' and different customer driving cycles.

a) Capacity degradation for field driving cycle 'A' for 20-80% SOC

The field driving cycle 'A' is fed into the vehicle and the obtained vehicle battery current is fed into the ageing model using the Complete RMS and Discretized RMS methods. The resulting capacity degradation is as shown in Figure 4.9.

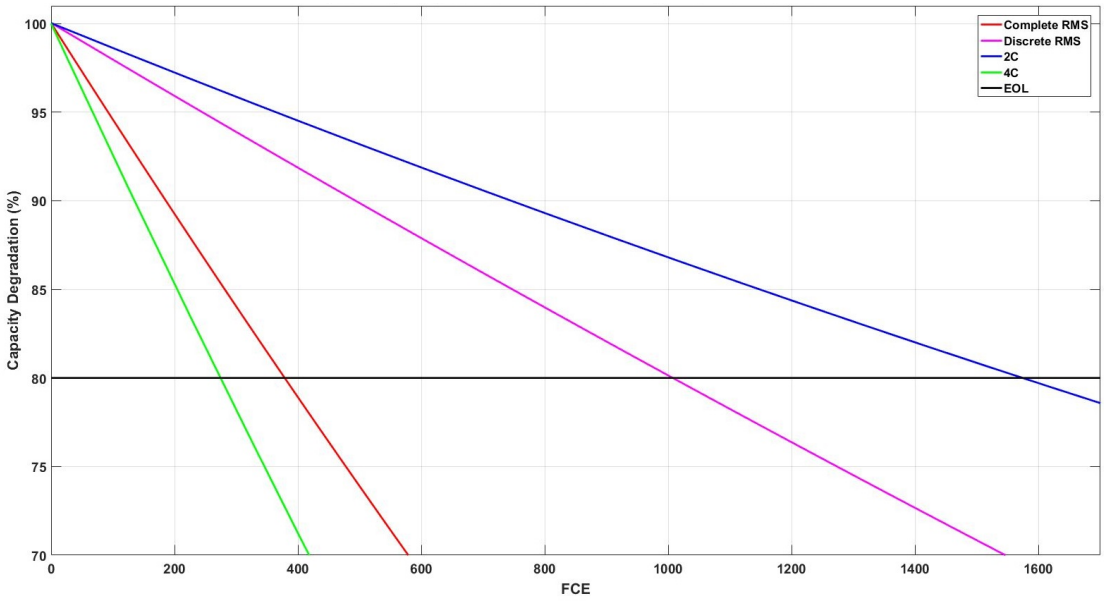

Figure 4.9: Capacity degradation for field driving data 'A' for 20-80% SOC

Using the Complete RMS method gives an RMS current of 89A which is around 3.4C. In the Discretized RMS method, the field drive cycle 'A' is divided into five different intervals with C-rates lying between 2.4C and 3.8C.The results are plotted with the capacity degradation at constant 2C and 4C for 20-80% SOC as shown in Figure 4.9. As expected, the ageing curve due to RMS methods lie in between the 2C and 4C curves.

It can be observed from Figure 4.9 that with the Complete RMS the EOL is reached at 380 FCEs, while the Discretized RMS results in 1008 FCEs. In reality, the actual vehicle battery will be stressed with discharging rates corresponding to the various decelerations and constant speeds instead of just one RMS value which is more degrading (in this case). From the above, it can be concluded that for dynamic drive cycles, using the Discretized RMS method is more beneficial in predicting the actual battery capacity degradation than using the Complete RMS method.

b) Capacity degradation for different customer driving patterns

The battery ageing is next studied for a driving data from an actual vehicle collected by the research project 'Bildatabasen'. This extensive driving data is scaled by half and 1.7 times to analyse three different driving scenarios namely I, II and III respectively, each having an average velocity of 23.8 km/h (I), 47.6 km/h (II) and 79 km/h (III). Figure 4.10 shows the speed profile of the original driving cycle II.

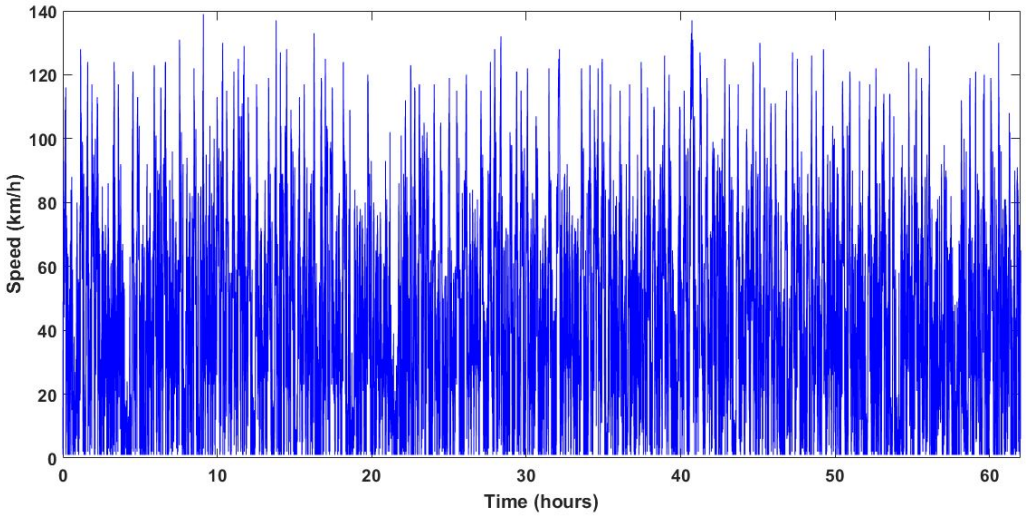

Figure 4.10: Speed profile of the Bildatabasen driving cycle II

These driving patterns are fed into the vehicle model and in turn the ageing model using the Discretized RMS method to study the battery capacity degradation under these scenarios. Figure 4.11 shows the capacity degradation for driving patterns I, II and III.

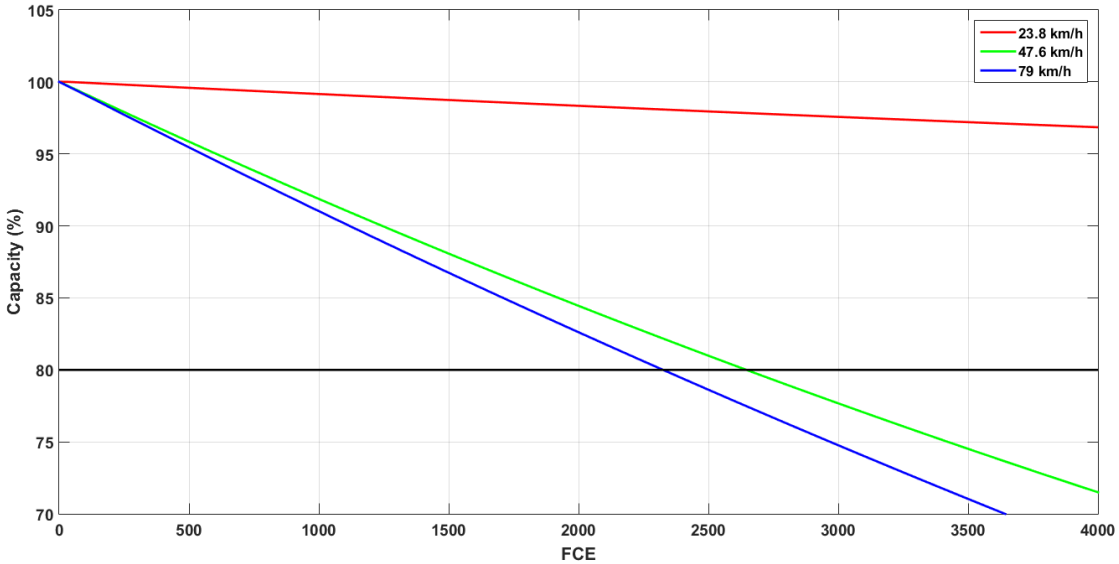

Figure 4.11: Capacity degradation for different customer driving patterns

It can be assumed that the battery of an electric vehicle has a lifetime of about 20,000 km/year and 8 years when used at an average speed of 77 km/hour. Thus, the battery would last for a total of approximately 2080 hours. Based on this, the battery life time (hours) can be calculated for different average velocities as mentioned in Table 4.1.

Figure 4.11 shows that for the driving pattern I, the capacity degradation is slow. Whereas for II and III, the EOL occurs at 2640 and 2300 FCEs respectively. This can then be compared and verified with the actual battery life in an electric vehicle as shown in Table 4.1. Table 4.1 shows that the battery lifetime (hours) calculated from the simulation are almost in line with the actual lifetime for the three driving scenarios considered.

Table 4.1: Battery EOL for customer driving patterns I, II and III

Cycle No.	Average Speed (km/h)	FCE from Simulation	EOL(hours) from Simulation	EOL(hours) from actual driving
I	23.8	N.A	N.A	N.A
II	47.6	2640	3432	3360
III	79	2300	1930	2027

Figure 4.11 illustrates that high speed driving accelerates the capacity degradation. The battery life lasts longer when the vehicle is driven at a lower speed as in the scenario I. This is because higher speed of the vehicle requires larger current from the battery. This means that the battery is getting discharged at a higher C-rate, which in turn speeds up the ageing process, causing the EOL to be reached earlier.

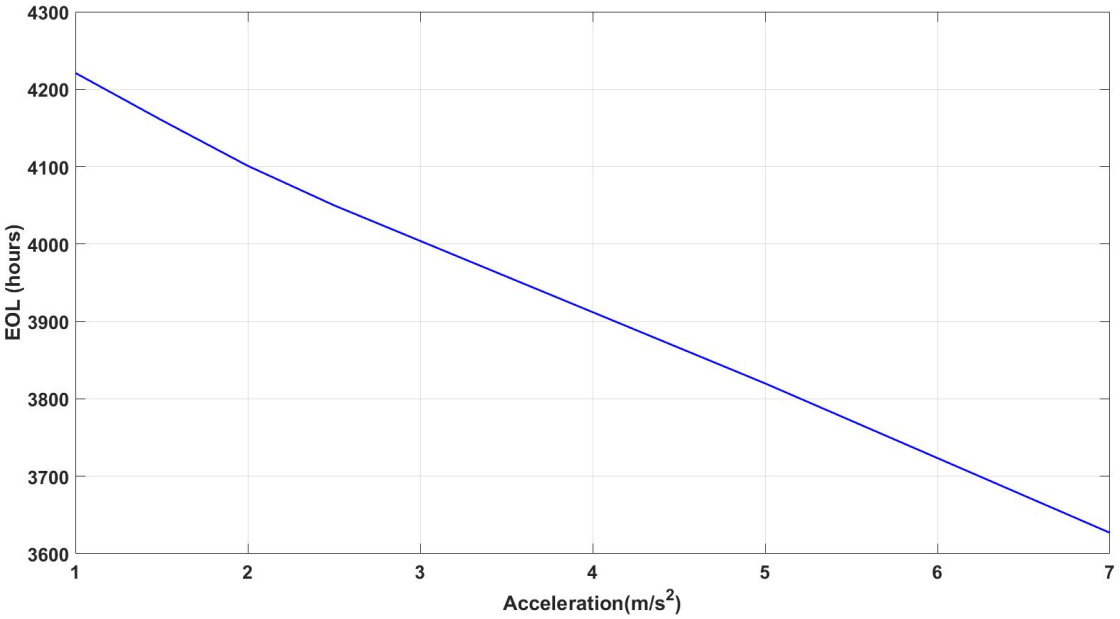

Figure 4.12: EOL for different accelerations for Bildatabasen driving cycle II

Figure 4.12 shows the EOL (in hours) for different acceleration limits for driving cycle II. It can be observed that driving a vehicle at higher acceleration of 7m/s results in EOL being reached earlier as compared to lower acceleration of 2m/s. It can be inferred that battery life time can be increased if the vehicle is driven at low accelerations.

Chapter 5

Conclusions

In this thesis work, the vehicle and battery ageing model have been built and integrated to study the impact of various driving scenarios on the battery lifetime. The vehicle model closely represents the behaviour of the PHEV test vehicle (the Electric Mode) and hence provides a good estimate of parameters such as the battery current, battery SOC, electric motor power etc.

A battery ageing model dependent on the C-rate and SOC is developed. For a constant C-rate, the capacity degradation is more severe at higher SOC levels (beyond 60%) than the lower ones. For a constant SOC window of 20-80%, the fast charging and discharging show a more rapid ageing compared to slow charge and discharge rates. The battery EOL is reached at 1600 FCEs for 2C and 200 FCEs for 4C. Thus, by doubling the C-rate, the battery life-time is reduced by 87% for 20-80% SOC. Also, the capacity degradation for 10% DODs at different SOC levels and different C-rates (1C, 2C and 4C) shows that the C-rates have a bigger impact on ageing in higher SOC windows (60-70%) as compared to lower SOC windows ageing (10-20%). Thus, it can be inferred from these results that fast charging and discharging have a more detrimental impact on the battery lifetime at higher SOC levels.

The vehicle and the battery ageing models are integrated and three different customer driving scenarios with different average speeds are analyzed. The study shows that the higher the average speed of the vehicle, the more is the battery stressed. A vehicle driving at an average speed of 79km/hour is likely to reach its battery's end of life much earlier as compared to a vehicle driving with an average speed of 23.8km/hour. Also, reducing the acceleration limits from $7m/s^2$ to $2m/s^2$ results in 13% increase in the battery life. Thus it can be concluded that an economical driving will slow down the ageing and prolong the battery lifetime.

Chapter 6

Future work

During the progress of this Thesis work several aspects have been identified that require further work for increasing the accuracy of the battery ageing analysis.

For building a more accurate vehicle model, the impact of temperature could be considered in the model. More data needs to be gathered to fine tune the vehicle parameters such as the aerodynamic drag and rolling friction coefficients C_d and C_r respectively.

The impact of temperature could also be included in the battery ageing model. More tests for various DODs such as 20%, 40% etc. could also be done to improve the model functioning at different DODs and SOC windows. In an actual driving, there are generally pauses which gives time for the battery to recover. Tests with an additional synthetic constant current (CC) driving cycle with pauses could be helpful in understanding the battery ageing. This would allow a more rational comparison between the CC and dynamic cycles.

The discrete RMS method used for integrating the vehicle and the battery ageing model has a major limitation. Its accuracy is highly dependant on the length of the discretization interval which in turn needs to be optimized for each type of driving scenario. More sophisticated techniques such as the Rainflow count method could also be implemeted and analyzed for more promising results. Battery ageing data of the actual vehicle could also be collected for more accurate verification of the ageing model.

The fine-tuned vehicle and battery ageing models could further be used to define realistic usage restrictions or battery control functions in a real vehicle and how it would impact the battery ageing and benefit the customers.

———-.

References

[1] www.electriccarsreport.com/2013/01/pike-forecasts-1-8m-evs-on-european-roads-by-2020

[2] Ageing mechanisms and how to prolong battery life in vehicle and energy storage applications.

[3] https://www.theguardian.com/sustainable-business/2017/aug/10/electric-cars-big-battery-waste-problem-lithium-recycling.

[4] https://www-tandfonline-com.proxy.lib.chalmers.se/doi/full/10.1080/10643389.2013.763578?scroll=topneedAccess=true.

[5] Lino Guzzella, Antonio Sciarretta, "Vehicle Propulsion Systems: Introduction to Modeling and Optimization". Springer, third edition.

[6] Olivier Tremblay, Louis-A. Dessaint and Abdel-Illah Dekkiche, “A Generic Battery Model for the Dynamic Simulation of Hybrid Electric Vehicles”, Vehicle Power and Propulsion Conference (VPPC) 2007, IEEE, 2007.

[7] Evelina Wikner, “Lithium ion Battery Aging: Battery Lifetime Testing and Physics-based Modeling for Electric Vehicle Applications,” Thesis for the degree of licentiate, Chalmers University of Technology, 2017.

[8] J. Groot, “State-of-health estimation of Li-ion batteries: Ageing models,” Ph.D. dissertation, Chalmers University of Technology, 2014.

[9] Emma Grunditz, "Design and assessment of Battery electric vehicle powertrain with respect to performance, energy consumption and electric motor thermal capability", Ph.D. dissertation, Chalmers University of Technology, 2016.

[10] Avnish Narula, "Modeling of Ageing of Lithium Ion Battery at Low Temperatures", Master thesis, Chalmers University of Technology, 2014.

[11] David Fernandez, "Model Building and Energy Efficient Control of a Series-Parallel Plug-in Hybrid Electric Vehicle", Master thesis, Chalmers University of Technology, 2016.

[12] J. Groot, "State-of-health estimation of Li-ion batteries: cycle life test methods", Licentiate thesis, Chalmers University of Technology, 2012.

[13] M. B. K. D. J¨urgen Remmlinger, Simon Tippmannb, “Low-temperature charging of lithium-ion cells part II: Model reduction and application,” Journal of Power Sources, December 2013.

[14] V. et al, “Ageing mechanism in li-ion batteries,” Journal of Power Sources, March 2005.

[15] S. T. et al, “Low-temperature charging of lithium-ion cells part I: Electrochemical modeling and experimental investigation of degradation behavior,” Journal of Power Sources, December 2013.